2-1-2013

Evaluation of the Complementary Relationship Using Noah Land Surface Model and North American Regional Reanalysis (NARR) Data to Estimate Evapotranspiration in Semiarid Ecosystems

W. Thilini Jaksa
Boise State University

Venkataramana Sridhar
Boise State University

Justin L. Huntington
Desert Research Institute

Mandar Khanal
Boise State University

 DOI: 10.1175/JHM-D-11-067.1

Evaluation of the Complementary Relationship Using Noah Land Surface Model and North American Regional Reanalysis (NARR) Data to Estimate Evapotranspiration in Semiarid Ecosystems

W. THILINI JAKSA AND VENKATARAMANA SRIDHAR

Department of Civil Engineering, Boise State University, Boise, Idaho

JUSTIN L. HUNTINGTON

Division of Hydrologic Sciences, Desert Research Institute, Reno, Nevada

MANDAR KHANAL

Department of Civil Engineering, Boise State University, Boise, Idaho

(Manuscript received 8 June 2011, in final form 15 October 2012)

ABSTRACT

Estimating evapotranspiration using the complementary relationship can serve as a proxy to more sophisticated physically based approaches and can be used to better understand water and energy budget feedbacks. The authors investigated the existence of complementarity between actual evapotranspiration (ET) and potential ET (ET_p) over natural vegetation in semiarid desert ecosystems of southern Idaho using only the forcing data and simulated fluxes obtained from Noah land surface model (LSM) and North American Regional Reanalysis (NARR) data. To mitigate the paucity of long-term meteorological data, the Noah LSM-simulated fluxes and the NARR forcing data were used in the advection–aridity (AA) model to derive the complementary relationship (CR) for the sagebrush and cheatgrass ecosystems. When soil moisture was a limiting factor for ET, the CR was stable and asymmetric, with b values of 2.43 and 1.43 for sagebrush and cheatgrass, respectively. Higher b values contributed to decreased ET and increased ET_p, and as a result ET from the sagebrush community was less compared to that of cheatgrass. Validation of the derived CR showed that correlations between daily ET from the Noah LSM and CR-based ET were 0.76 and 0.80 for sagebrush and cheatgrass, respectively, while the root-mean-square errors were 0.53 and 0.61 mm day^{-1}.

1. Introduction

Evapotranspiration (ET) is an important component for both energy and water cycle assessments at local, regional, and global scales. South central Idaho is a semiarid region characterized by low precipitation, shrubland, and grassland ecosystems. Water supply in the area largely depends on the runoff from mountains surrounding the Snake River Plain, and the groundwater recharge is fulfilled by rain and melting snow during winter and the early spring (Kjelstrom 1995). The nominal summer precipitation is generally lost through canopy-intercepted evaporation, soil evaporation, and plant transpiration and therefore is not available to recharge the soil column. When the soil is dry, water-limited shrub and grassland vegetation become water stressed and will close their stomata, thereby restraining transpiration (Monteith 1975; Avissar and Pielke 1991). A combination of limited soil moisture and stomatal control diminishes the total ET during the summer from these natural ecosystems. As a sink term in the water balance and land surface energy balance, ET is not only important for the water resources management but also in land–atmosphere feedbacks through ET on a regional scale. Raupach (1998) identified ET as an important process that links the land and atmosphere. The ability for regional atmospheric and general circulation models to represent the land and atmosphere feedbacks is critical for understanding current and future climate

Corresponding author address: Venkataramana Sridhar, Department of Civil Engineering, Boise State University, 1910 University Dr., ERB 3133, Boise, ID 83725-2060.
E-mail: vsridhar@boisestate.edu

DOI: 10.1175/JHM-D-11-067.1

and water resource scenarios in this region, where regional warming and shifts in snowmelt timing have been documented (Barnett et al. 2005; Mote 2006; Clark 2010; Bureau of Reclamation 2011; Jin and Sridhar 2012).

ET can be measured in the field by a weighing lysimeter and estimated by various methods such as eddy covariance, Bowen ratio, and scintillometers (Rana and Katerji 2000; Beyrich et al. 2002; Meijninger et al. 2006; Samain et al. 2011). These water and energy balance approaches are always costly and labor intensive and require extensive maintenance. Therefore, there are several empirical and analytical methods commonly used in hydrologic models to simulate ET. Computation of ET in these models at field scale is based on theories and equations that have been derived, such as the water balance and energy balance methods (Monteith 1973; Rana and Katerji 2000). Upscaling of ET estimates from field scale to regional scale by preserving heterogeneity has been quite successful over the past decade (Kavvas et al. 1998; Sridhar et al. 2003). In water balance studies, ET is often computed as the difference between precipitation and runoff at the basin scale or limited by soil moisture functions for smaller-scale applications (Walter et al. 2004; Sridhar and Nayak 2010; Shukla et al. 2011). Energy balance–based land surface models (LSMs) and satellite-based models (Allen et al. 2007a,b; Alfieri et al. 2009; Tang et al. 2009; Tang et al. 2010) are also widely used to estimate ET. In this study, the objective is to develop the complementary relationship (CR), which is based on model predictions of ET for the most common land cover types, sagebrush and cheatgrass, present in the semiarid ecosystems of Idaho. Observed ET data are not available on a regional scale. Therefore, if there is another effective method available to estimate ET, it is best to cross-validate the estimates of ET by using the North American Regional Reanalysis (NARR) (Mesinger et al. 2006) data; it provides us with the baseline estimates of potential and actual ET to derive the relationship. NARR data are derived by a coupled model, and thus, the land–atmospheric coupling is expressed through precipitation updates and not the surface. However, the spatial resolution of NARR is too coarse to represent the heterogeneity in the land cover over this region. Therefore, the high-resolution land data assimilation system (HRLDAS) platform of the Noah LSM was adopted only to disaggregate the NARR data to a finer resolution.

2. Theoretical background on complementary relationship

Among many methods to quantify ET, an approach derived from the CR is gaining renewed attention as it is a relatively simple method to calculate actual evapotranspiration (Brutsaert and Stricker 1979; Hobbins et al. 2001; Oudin et al. 2005; Xu and Singh 2005; Pettijohn and Salvucci 2009; van Heerwaarden et al. 2010; Crago et al. 2010; Huntington et al. 2011). This complementary relationship between the actual ET and the potential ET (ET_p) was first proposed by Bouchet (1963) and was based entirely on heuristic arguments. This is again built upon the land–atmosphere feedback mechanism between actual evaporation and potential evaporation, where potential ET decreases as there is more moisture in the near-surface boundary layer because of increases in actual evapotranspiration (Fig. 1). Estimating ET using this method is easy compared to the other methods because it requires only a standard set of meteorological variables. The difference between the Penman (1948) and Penman–Monteith equations are the use of resistance terms. Since ET_p is calculated using Penman (1948), which does not require aerodynamic or canopy resistance terms, it avoids the extremely cumbersome process of aerodynamic and canopy resistance parameter calibration (Huntington et al. 2011). Furthermore, the resistance terms used in the Penman–Monteith equation, aerodynamic and surface resistance, are vegetation specific, and we do not have those two parameters specific to the vegetation type. A cursory calculation of ET_p for sagebrush using both of the methods showed that ET from Penman (1948) was slightly higher; however, the differences were insignificant. Additionally, estimation of ET in the precipitation-limited regions of the Snake River Plain is constrained by the spatiotemporal distribution of

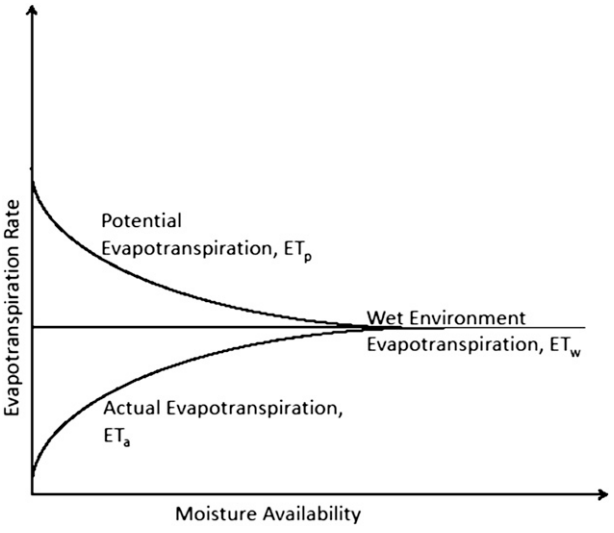

FIG. 1. Schematic diagram of a general complementary relationship between ET and ET_p. Under similar available energy scenarios, ET increases when ET_p decreases as we move along the abscissa with increases in soil moisture.

weather stations to employ traditional ET approaches, and there is a lack of observed long-term surface flux measurements to calibrate certain parameters and validate the methodologies.

Under the CR assumption, when there is enough soil moisture and when only the available energy is a limiting factor, ET increases and reaches ET_p. This condition is denoted by a term called equilibrium ET (ET_w). The quantity ET_w is the ET that occurs from a regionally wet surface. Under soil moisture–limited conditions and when the available energy is not a limiting factor, ET decreases below ET_w, creating a certain amount of energy available (Q):

$$ET_w - ET = Q. \quad (1)$$

This available energy Q then causes increase in ET_p by an amount of Q:

$$ET_w + Q = ET_p. \quad (2)$$

This increase in ET_p is mainly caused by the increased air temperature from the available energy Q and decreased humidity due to decreased ET. Combining (1) and (2),

$$ET + ET_p = 2ET_w. \quad (3)$$

The above equation indicates a symmetric CR. That is, one unit decrease in ET results in one unit increase in ET_p. Figure 1 shows the schematic of theoretical complementary relationship. A general form of CR can be written as

$$(1 + b)ET_w = ET_p + (b \times ET), \quad (4)$$

where b is a proportionality constant. In a symmetric CR, b becomes 1. However, Kahler and Brutsaert (2006) explained that b can take values greater than 1 when pan evaporation is used. This happens because of the additional energy received from the exposed sides, as well as the bottom of the pan, and a larger water vapor transfer coefficient from local advection because of its small size. The study by Pettijohn and Salvucci (2009) using terrestrial and pan evaporation was also in agreement with Kahler and Brutsaert (2006) with a b value of approximately 5. Brutsaert and Parlange (1998) have explained the evaporation paradox using the CR theory, observing the declining trend in pan evaporation while temperatures were rising. Hobbins et al. (2004) proved the argument put forth by Brutsaert and Parlange (1998) on the CR by relating the pan ET and actual ET based on trends in pan ET and the large-scale water balance-based actual ET for 655 basins across the conterminous United States.

There are several models based on CR to predict the actual ET, including the advection–aridity (AA) model (Brutsaert and Stricker 1979), the complementary relationship of areal evaporation (CRAE) model (Morton 1983), and the complementary relationship model (Granger and Gray 1989). Xu and Singh (2005) evaluated the performance of the above three models over three different regions. They found that locally calibrated parameter values improved the model performance. It is clear that soil moisture also controls the climate variables (temperature, sensible, and latent heat flux) and can impact the CR as reported by Xu and Singh (2005). In a similar way, for the semiarid regions of Idaho, the influence of soil moisture on CR-based ET can be significant. Hobbins et al. (2001) also showed a poor performance of the original AA model. By reparameterizing the wind function used in the calculation of potential ET and recalibrating the Priestley–Taylor coefficient in the wet environment ET formulation, estimates of the annual average ET were improved. Ozdogan et al. (2006) used a mesoscale climate model and meteorological data to evaluate the CR between the potential and actual ET. In addition to the CR, they found that wind speed and stability effects are the main factors in maintaining the complementarity.

3. Approach

Considering the importance of estimating ET in partitioning the water budget where the data are limited, this study tested whether the relationship between ET_p and ET was complementary, and if so, whether this method could be used in a prognostic approach to predict ET for natural vegetation in south central Idaho. Cold winters and hot, dry summers are common in this area. Average annual precipitation ranges from 200 to 250 mm, and the mean annual air temperature range is 5°–10.9°C, with July being the warmest month with highest evaporation (Kjelstrom 1995). During the peak summer months, natural ecosystems, including sagebrush and cheatgrass communities considered in this study, are very dry and ET is very low. The Noah LSM–predicted ET was utilized instead of measured ET to evaluate if the CR can be derived for the two dominant cover types, sagebrush and cheatgrass, for a certain period. It should be noted that we verify the CR in a modeling world with another model-derived product, NARR, being the driver by itself in our investigation. Subsequently, the derived CR was used as a predictor of actual ET from ET_p and wet surface evaporation. This was performed not by using any in situ weather or flux data but with only meteorological

data obtained from NARR spatially interpolated by HRLDAS and the Noah land surface model-simulated ET over the period 1979–2010. Forcing data obtained from NARR were used to compute ET_p and ET_w, and computed ET_p and ET_w, along with Noah LSM ET, were subsequently used to derive the CR between 2001 and 2010. Validation of this relationship was performed for the growing season between 1981 and 2000 to test if the derived relationship could quantify ET precisely for other years. As mentioned before, the scarcity of meteorological measurements is a drawback in characterizing the near-surface boundary layer feedbacks of the natural vegetation. Therefore, NARR data (Mesinger et al. 2006) were used in this study, which allowed for an evaluation of NARR forcings and their utility in establishing a complementary relationship to predict ET for similar and data-poor regions elsewhere.

NARR was developed at the Environmental Modeling Center (EMC) of the National Centers for Environmental Prediction (NCEP). Based on ground observations, NARR was generated by the NCEP Eta model using its data assimilation system and a recent version of the Noah LSM (Mesinger et al. 2006; Luo et al. 2007). NARR data come as three-hourly composites and covers the North American domain with a horizontal resolution of 0.3° (32 km). A major weakness of this dataset when applying it to water resource management is its coarse spatial resolution. It is too coarse to represent the vegetation heterogeneity. As ET largely depends on vegetation types and categories, the coarse spatial resolution in NARR is not suitable to represent the land use heterogeneity of the land. Therefore, the HRLDAS platform was used to spatially interpolate NARR in order to obtain meteorological variables at a higher spatial resolution, which would subsequently match with the spatial resolution of Noah LSM-predicted ET. The use of higher spatial resolution data was also important in representing the vegetation distribution in the region. Ozdogan et al. (2006) used a coupled version of the Noah LSM combined with meteorological data to show the existence of CR. Both Noah LSM-simulated fluxes (net radiation and ground heat flux) and downscaled meteorological data (minimum, maximum, and mean temperature; wind speed; and vapor pressure) obtained from the uncoupled Noah LSM were used in deriving the CR. Furthermore, Noah LSM-simulated ET using NARR data was available only at the 32-km resolution, which was not suitable for our analysis. It is partly because of the coarse spatial resolution of NARR data, considered as one of the major constraints to study local-scale effects. Therefore, ET was computed from Noah LSM at 2-km resolution. Estimating ET using the CR approach is relatively simple compared to that of implementing a land surface hydrology model such as the Noah LSM. Also, once the relationship was derived, CR became independent of the plant–land cover properties and required only meteorological data. In case of Noah LSM, it required several parameters, including vegetation and soil conditions. Generally, estimating these relevant parameters and making them pertinent to the study area is feasible, but it is based on a rigorous calibration exercise and there are uncertainties associated with the estimated parameters. In situations where sufficient data do not exist, available parameters are generally used by the model, and the usage could introduce uncertainties in the model estimates. In this study, it was preferred to compare the Noah LSM performance and the applicability of NARR data for the study area. Also, we demonstrate the utility of the CR method to get an independent estimate of ET, as it was perceived as one of the most contentious variables in the water user community and by water managers in the region.

Testing and application of CR derived from NARR was expected to prove valuable for estimating ET under historical conditions. If the focus was to evaluate the predictability of ET by the CR technique on the basis of field observations, then it would be reasonable to make conclusions about the performance of NARR in estimating ET against CR; however, that was not the emphasis of this study. The main goal of this research was to derive CR for the vast expanse of natural vegetation ecosystems in southern Idaho during the growing season. Studies using CR for arid and semiarid regions (Oudin et al. 2005; Xu and Singh 2005; Yang et al. 2006; Huntington et al. 2011) showed that estimating ET for the growing season was plausible. A well-formulated, physically based ET estimation technique with fewer parameters, such as the CR approach used in this study, has the potential to fill a critical gap in energy and water balance partitioning studies.

4. Noah land surface model

The Noah land surface model was used in this study to compute the actual ET that served as a proxy for observed ET in deriving the CR. The derivation of CR also enabled us to evaluate if the Noah LSM-derived ET was indeed complementary with the NARR-based near-surface weather variables. The Noah LSM is a widely recognized model, originally developed by Pan and Mahrt (1987), and has been constantly subjected to improvements. Some of them are modifications in the canopy resistance formulation (Chen et al. 1996), bare soil evaporation and vegetation phenology (Betts et al. 1997), surface runoff infiltration (Schaake et al. 1996), thermal roughness length treatment in the surface layer

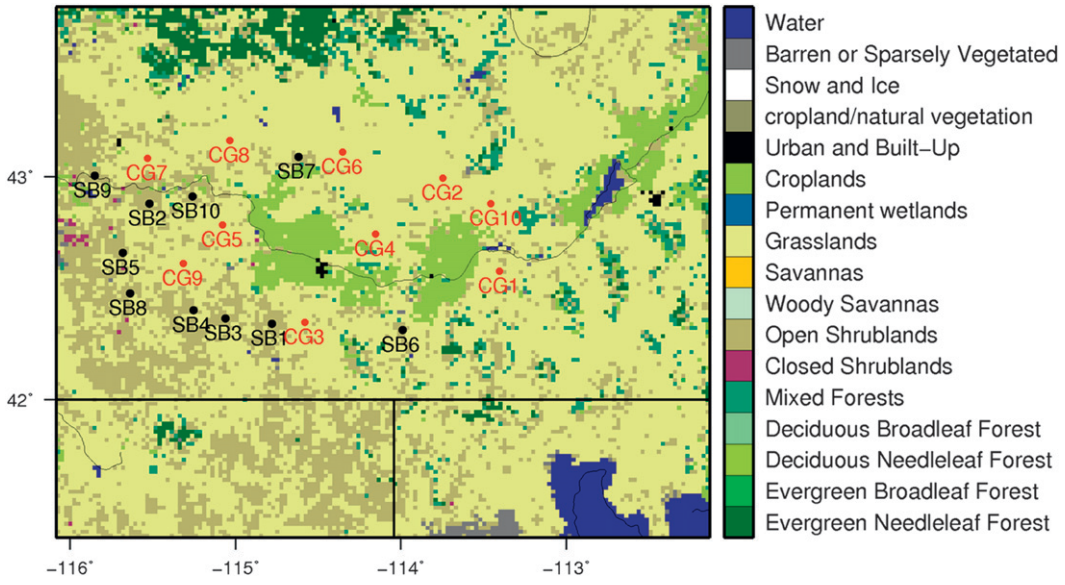

FIG. 2. Vegetation map of the study area at 2-km resolution adopted from the MODIS-based classification. Sites with sagebrush are marked with black circles and those with cheatgrass with red circles.

exchange coefficients (Chen et al. 1997), and the addition of frozen soil physics (Koren et al. 1999). The Noah LSM has been used in many studies and has shown promising results when compared with surface flux measurements. Sridhar et al. (2002) validated the simulations with surface flux measurements in Oklahoma, which showed reasonably good correlations with low bias and error. It was shown that the Noah LSM was able to capture the surface heterogeneity when the surface flux maps from the Noah LSM were compared with both surface and aircraft measurements by Chen et al. (2003). Radell and Rowe (2008) analyzed the influence of shallow groundwater on the Noah LSM-simulated surface fluxes in the Sand Hills of Nebraska using field observations. Their results revealed that it performed well for the dry sites where the water table had negligible influence on the root zone.

The Noah LSM has four soil layers, one canopy layer, and one snow layer. The depths of the soil layers from the surface are 10, 40, 100, and 200 cm. HRLDAS runs the Noah LSM in an uncoupled mode, which was developed to address the issues related to initializing soil moisture and temperature fields (Chen et al. 2007). The Noah LSM has been developed to be compatible with the Weather Research and Forecasting (WRF) model, in which the grid configuration within the model and retrievals of constant fields, like soil and land use categories, as well as the green vegetation fraction, are done by using the WRF preprocessing system (WPS). More details about the Noah LSM physics and HRLDAS platform can be found in Chen et al. (1996) and Chen et al. (2007), respectively. This study was performed using HRLDAS version 3.1 along with the Noah LSM version 3.2.

5. Data and methodology

a. Model domain and configuration

The Noah LSM domain is shown in Fig. 2. It is located roughly between 41.37°N and 43.75°N and between 112.13°W and 116.15°W, enclosing a land area of 85 536 km^2. The main land cover types in the area are shrublands and grasslands (Fig. 2). According to the Moderate Resolution Imaging Spectroradiometer (MODIS)–based land cover classification, the dominant land cover type is grasslands, which is about 71% of the model domain. Shrublands cover 15% of the area as the second-most dominant category within the model domain. The model domain was represented as 2-km grids using the WPS program. All of the meteorological forcing data, and other data for initialization, were interpolated spatially into 2 km and temporally into 1 h in the HRLDAS platform. A 10-yr period was chosen between 2001 and 2010 for deriving CR, and a 20-yr period between 1981 and 2000 was chosen for validating the results. Two years, 1979 and 1980, were treated as a spinup period and were excluded from the analysis. A spinup period of one year was recommended for HRLDAS by a previous study (Chen et al. 2007). To avoid any sampling error, 10 cells distributed within the model domain were chosen for the subsequent CR analysis for each

vegetation type (sagebrush and cheatgrass), and it was assumed that those 10 cells could represent the total area of that particular vegetation in the domain. Simulation was performed at the hourly time step using the three-hourly NARR data. For deriving the CR, all of the 10 cells were used for the whole period to compute an average b value. However, obtaining higher temporal resolution was not the focus, since the results were aggregated to daily and seasonal totals. A particular interest was to represent the land use heterogeneity in the region, and in order to achieve this, Noah LSM and the HRLDAS platform were implemented with 2-km resolution. The recent version of the Noah LSM model (version 3.2) was used with the default parameters. The original spatial resolution of NARR was 32 km, which was too coarse to represent the vegetation distribution. Land use and land cover data have significant impacts in estimating evapotranspiration from any area. A higher-resolution land cover map (30″ resolution MODIS-based land surface characterization with 20 categories) was therefore used in the offline Noah LSM to simulate ET.

Implementation of a coupled model that links the surface and atmosphere dynamically can be computationally demanding. As stated earlier, our goal was to use modeled ET to derive and validate the CR without the need for field observations of ET or weather variables. The offline model was a good alternative, given the ability of the model to predict fluxes over the growing season in semiarid regions. In the uncoupled mode, the Noah LSM should be provided with input forcings of atmospheric variables from the NARR dataset used in our simulations. The required near-surface forcing fields were air temperature (K), atmospheric mixing ratio (kg kg^{-1}), u and v components of the horizontal wind (m s^{-1}), surface pressure (Pa), precipitation rate (kg m^{-2}), and downward shortwave and longwave radiation flux at the surface (W m^{-2}). The Noah LSM was also provided with the initial conditions of soil temperature (K) and soil moisture (kg m^{-3}) at each model soil layer, canopy water content, skin temperature, and water equivalent of accumulated snow depth. These data were obtained from the NARR dataset, which is explained in section 6a.

In addition to forcing and initialization fields, the Noah LSM needed static and time varying data to define soil, vegetation, and geographical details. These fields were obtained through the WPS, and they included vegetation and soil types, minimum and maximum green vegetation fraction for a typical year, time invariant deep soil temperature, and monthly green vegetation fraction. The green vegetation fraction was based on 5-yr monthly averages of normalized difference vegetation index (NDVI), which were calculated using 0.15° Advanced Very High Resolution Radiometer (AVHRR) data (Chen et al. 2007).

b. Data preparation for the AA model

Simulated actual $\mathrm{ET}_{\mathrm{Noah}}$ was obtained from the Noah LSM for the years between 2001 and 2010 in order to examine the CR over the two vegetation types. The ET_p was calculated at daily time steps using the Penman (1948) approach, with the Rome wind function following the Brutsaert and Stricker (1979) formulation of the AA as

$$\mathrm{ET}_p = \frac{\Delta Q_n + \gamma E_a}{(\Delta + \gamma)}, \tag{5}$$

where Q_n is the available energy (R_n − GH) in water-depth equivalent (mm day^{-1}), R_n is net radiation, GH is ground heat flux, Δ is the slope of the saturation vapor pressure at air temperature, γ is the psychrometric constant, and E_a is the drying power of air. Ground heat flux was simulated using the Noah LSM. The quantity E_a can be computed using Penman's original Rome wind function for a free water surface, which is given by

$$E_a = 0.26(1 + 0.54U)(e_s - e_a), \tag{6}$$

where U is the measured wind speed at 2 m (m s^{-1}), and e_s and e_a are the saturation and actual vapor pressure at air temperature, respectively. NARR 10-m wind speed and 2-m weather data of daily average temperature and vapor pressure and the Noah LSM output of daily average R_n and GH were used in (5) and (6). The Penman approach was preferred over the Penman–Monteith (Monteith 1973) because of the absence of aerodynamic resistance and stomatal resistance terms.

A normalization procedure was applied following Kahler and Brutsaert (2006) and Huntington et al. (2011) in order to obtain a universal relationship with a dimensionless formulation. This was achieved by dividing both $\mathrm{ET}_{\mathrm{Noah}}$ and ET_p by the wet environment evapotranspiration ET_w. Priestley and Taylor (1972) introduced an equation to estimate equilibrium ET under minimal advection. The Priestley–Taylor equation, as used in other CR studies (Brutsaert and Stricker 1979; Kahler and Brutsaert 2006) to compute ET_w, was used in this work as

$$\mathrm{ET}_w = \frac{\alpha \Delta Q_n}{(\Delta + \gamma)}, \tag{7}$$

where α is the Priestley–Taylor coefficient and is assumed to be 1.26. In arid areas the measured or simulated air temperature can be quite different than the representative wet environment air temperature and hence

can impact the calculation of Δ in Eq. (7). Because in wet environments the air temperature gradient is relatively small, wet environment air temperature usually can be approximated by the wet environment surface temperature (Huntington et al. 2011). Therefore, Δ was evaluated at wet environment surface temperature (T_e) following the method used by Szilagyi and Jozsa (2008) and Szilagyi et al. (2009). Huntington et al. (2011) showed the use of T_e in calculating the ET_w resulted in a symmetric CR and improved predictions of ET using the AA model for arid shrublands. The T_e was estimated using the Bowen ratio (B_o) by an iterative process from air temperature and vapor pressure data for a small hypothetical wet surface using the equation below:

$$B_o = \frac{H}{\mathrm{ET}_p} = \frac{Q_n - \mathrm{ET}_p}{\mathrm{ET}_p} = \gamma \frac{T_s - T_a}{e_s - e_a} \approx \gamma \frac{T_e - T_a}{e_s(T_e) - e_a}, \quad (8)$$

where H is the sensible heat flux; T_s and T_a are wet surface and measured air temperature, respectively; and $e_s(T_e)$ is the saturated vapor pressure taken at wet environment surface temperature.

Because of passing weather systems and the decoupling of the land surface with the near-surface boundary layer, it has been recommended that the CR not be applied to a time step less than 3–5 days (Morton 1983). However, in order to maintain a significant number of data to analyze a 7-day moving average of daily ET_{Noah}, ET_p and ET_w were computed centered at the fourth day. The computed dimensionless terms of ET_{Noah} and ET_p are

$$E_+ = \frac{\mathrm{ET}_{\mathrm{Noah}}}{\mathrm{ET}_w} \quad (9)$$

$$E_{P+} = \frac{\mathrm{ET}_p}{\mathrm{ET}_w}. \quad (10)$$

Equations (9) and (10) also can be written as a function E_{MI} ($E_{MI} = ET_{Noah}/ET_p$) as

$$E_+ = \frac{(1+b)E_{\mathrm{MI}}}{1 + bE_{\mathrm{MI}}} \quad (11)$$

$$E_{P_+} = \frac{1+b}{1+bE_{\mathrm{MI}}}, \quad (12)$$

where b is a proportionality constant of the CR shown in (4) and E_{MI} represents a moisture index and indicates the potential for ET from the land surface.

6. Results and discussion

a. Complementary relationship in the Noah LSM and NARR data

In this study, the simulated results of ET_{Noah} were analyzed to evaluate the CR between March and September 2001–2010. Winter months were excluded from the analysis because of passing weather systems and potential decoupling between the land surface and near-surface boundary layer. During winter months, ET_{Noah} was observed to be higher than ET_w for a few days, making E_+ more than 1, which could be attributed to advection effects, making the CR invalid during these periods. Huntington et al. (2011) showed that adding winter months resulted in scatter and asymmetry to the CR. Scatter in the E_+, impacted by the inclusion of winter periods, resulted in extremely low, energy-limited ET_w values and large ET_p values, possibly from dry windy conditions, which greatly increased the ET_p/ET_w ratio. Normalized terms of E_+ and E_{P_+} were computed by Eqs. (9) and (10) using ET_{Noah}, ET_p from Eq. (5), and ET_w from Eq. (7). Figure 3 shows the nonnormalized CR for the two locations selected for the period from March to November during 2001–10 (excluding winter months). Modeled ET_{Noah} showed a complementary behavior between the computed ET_p using NARR data and the Noah LSM output for the two natural vegetation sites, even before normalizing. Even though there is some scatter in the plot, ET_{Noah} and ET_p behaved complementarily; under high soil moisture conditions, ET_{Noah} increased and ET_p decreased by converging around 1–2 mm day^{-1}.

The normalized ET_{Noah} and ET_p in Fig. 4 clearly show this relationship with less scatter. However, after removing the winter period, E_+ showed values higher than 1 for some days, especially at the beginning of March and during October and November. It should be noted that the ratio of ET/ET_w should never be greater than 1 for conditions of no net advection. The ratio ET/ET_w became more than 1, especially in the fall and early spring months when soil moisture started influencing the surface energy budget. The main reason for a higher ET/ET_w ratio was because of higher ET that resulted from Noah LSM, not because of the NARR data used to calculate ET_w. Numerous studies have identified higher snowmelt rates in the uncoupled Noah LSM simulation (Ek et al. 2003; Mitchell et al. 2004; Jin and Miller 2007), especially in the early spring. Albedo and vegetation fraction have significant controls on high snowmelt rates (Jin and Miller 2007). This increased snowmelt rate caused overestimation of ET in the Noah LSM. Since the Noah LSM-simulated ET was used here to derive the CR, the periods where Noah LSM showed weak performance

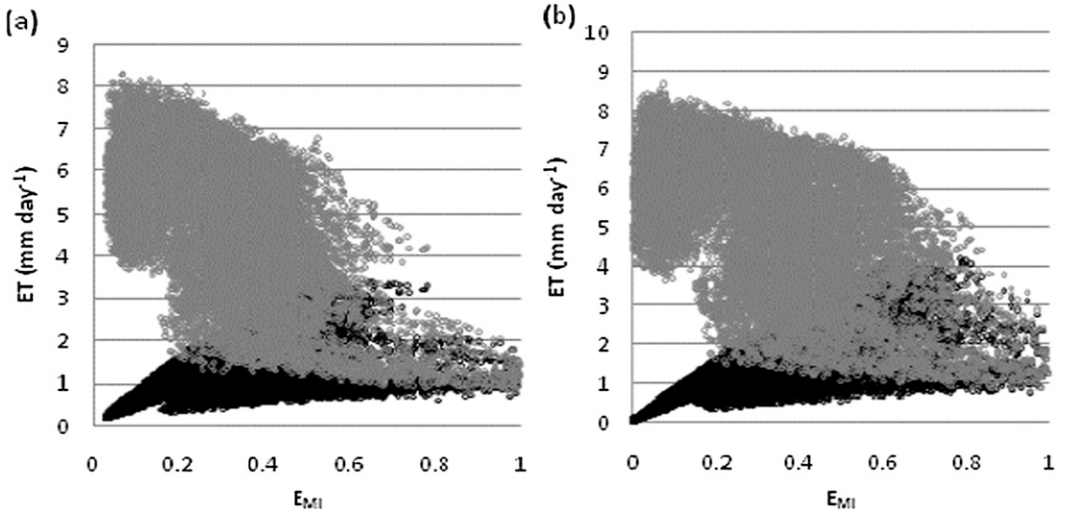

FIG. 3. The nonnormalized CR for the two vegetation types from all 10 cells for the period 2001–10: (a) sagebrush and (b) cheatgrass. Black circles indicate daily actual ET and gray circles indicate daily ET_p.

were carefully avoided. Results indicated that for a selected number of days in March, October, and November, ET_{Noah} was higher than ET_w by about 0.22 mm day^{-1} for sagebrush and 0.21 mm day^{-1} for grassland. The ET_w was a result of assuming unlimited moisture availability for evapotranspiration, while ET_{Noah} was subjected to both water and energy limitations, which should be always less than or equal to ET_w (i.e., $ET/ET_w \leq 1$).

Time series of E_+, E_{P_+}, and E_{MI} (Fig. 5) were analyzed along soil moisture conditions (Fig. 6) to examine possible causes for ET_{Noah} being greater than ET_w. Figure 5 shows that E_+ started having unrealistic values (>1) at the end of October for both the sites. The E_{P_+} was approximately stable around 2, until the end of September, and started fluctuating thereafter. By studying the hydroclimatology of the region, the main variation during September and October could be attributed to the beginning of the wetting season, which resulted in increased soil moisture conditions. Soil moisture in the first layer (0–10 cm) started to rise from 0.11 to 0.21 m^3 m^{-3} at the sagebrush site and 0.06 to 0.14 m^3 m^{-3} at the cheatgrass site following precipitation events in September (Fig. 6). This increased soil moisture, as simulated by the Noah LSM, caused a rise in ET_{Noah} due to increased direct evaporation and canopy evaporation. This increase was controlled when the soil moisture reached a limiting

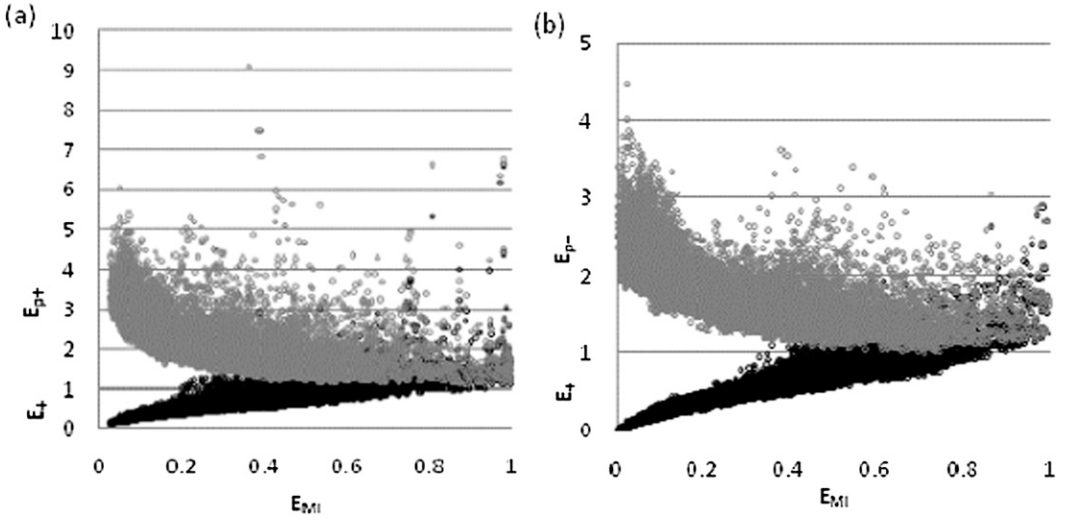

FIG. 4. The normalized CR for the three selected locations: (a) sagebrush and (b) cheatgrass. Black circles indicate E_+ and gray circles indicate E_{P_+}; E_+, E_{P_+}, and E_{MI} are dimensionless values.

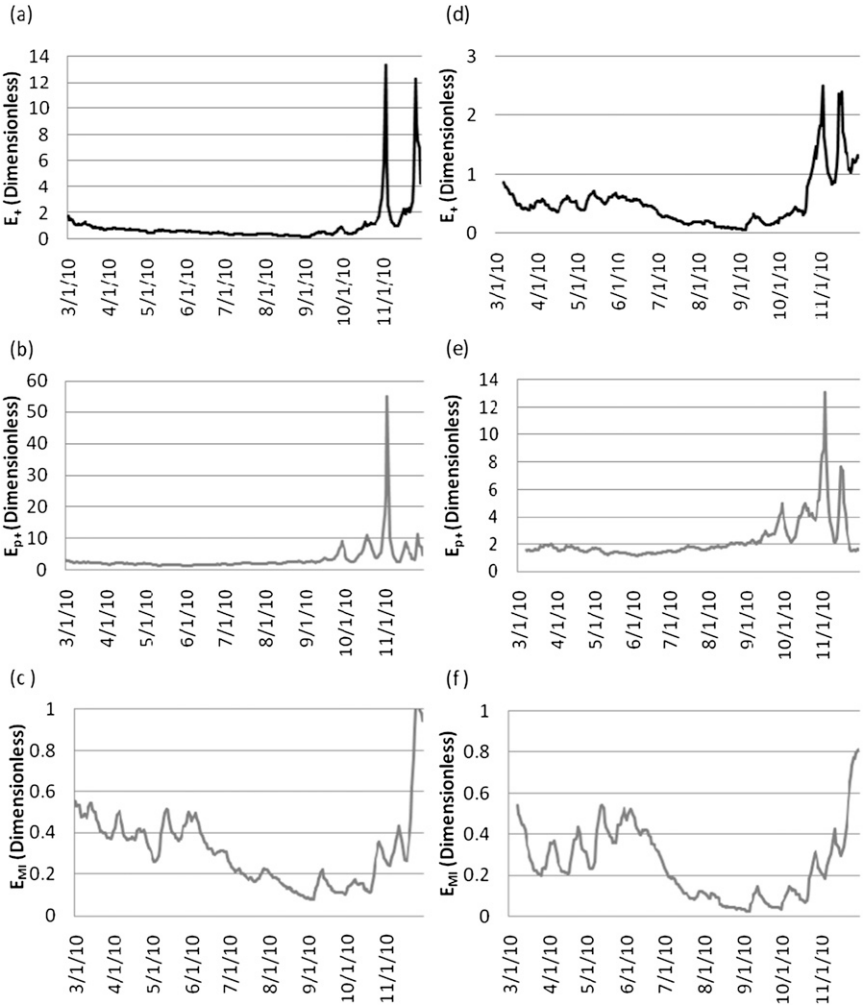

FIG. 5. Time series of (top to bottom) E_+, E_{P_+}, and E_{MI} for two sites: (a)–(c) sagebrush and (d)–(f) cheatgrass for 2010.

point. According to the CR, because of increases in ET with the precipitation, the resultant increase in atmospheric humidity should reduce ET_p at the next time step. Then $\mathrm{ET}_{\mathrm{Noah}}$ was computed as a factor of Noah-predicted ET_p, which was derived from a modified version of the Penman equation. Overestimation of ET_p from Noah LSM can lead to the overestimation of $\mathrm{ET}_{\mathrm{Noah}}$. Therefore, when compared against the ET_w, calculated by Priestley–Taylor equation, $\mathrm{ET}_{\mathrm{Noah}}$ was higher for selected days, causing E_+ to be greater than 1 during the end of October.

When the soil moisture was a limiting factor of ET, it was evident that the CR was stable for natural vegetation. On the other hand, when there was enough soil moisture (soil moisture was not a limiting factor for ET), the CR appeared to have a loose correlation, likely due to advection or the loose coupling between the Eta model and the NARR data as a result of coarse resolution (32 km), or perhaps overestimation of ET_p in the Noah LSM. However, this was not observed during the spring months (March–May), even though the soil was sufficiently wet with approximate soil moisture contents in the first layer of 0.26 $\mathrm{m}^3\ \mathrm{m}^{-3}$ for sagebrush and 0.2 $\mathrm{m}^3\ \mathrm{m}^{-3}$ for cheatgrass. Therefore, for further analysis and the derivation of CR for the two sites, days when $\mathrm{ET}_{\mathrm{Noah}}$ was higher than ET_w were not used. The period of 1 March to 15 September 2010 was chosen for further analysis.

b. *Estimation of CR for sagebrush and cheatgrass*

To evaluate the shape and degree of symmetry of the CR, the proportionality constant, b in Eq. (4), was evaluated using (9) and (10). The value of $\mathrm{ET}_{\mathrm{Noah}}$ was obtained from the Noah LSM, and ET_p was computed using Penman (1948) with the NARR weather data and the Noah LSM output. Values of b were found by minimizing

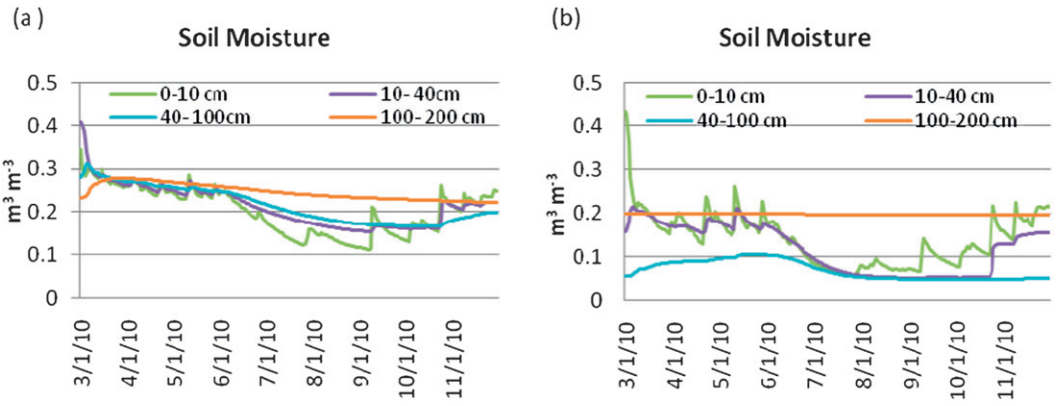

FIG. 6. Soil moisture at four soil layers for the two sites: (a) sagebrush and (b) cheatgrass obtained from the Noah LSM output.

the sum of the squared error between ''observed'' E_+ and E_{P_+} calculated by (9) and (10) and ''simulated'' E_+ and E_{P_+} using (11) and (12). It was found that b was 2.43 for sagebrush and 1.43 for cheatgrass, using T_e for computing ET_w (Fig. 7). Huntington et al. (2011) obtained a symmetric CR with $b = 1.008$ for phreatophyte shrub species (greasewood and rabbit brush) in eastern Nevada. However, in this study, the CR was not symmetric for the sagebrush site. The difference in b values between the sites is likely due to the treatment of evaporation and transpiration controls in Noah and Eta models, therefore impacting temperature and humidity fields in NARR, or because there is more net advection present at the sagebrush site than cheatgrass site. Szilagyi (2007) explained that asymmetry in CR occurs in drying environments with increasing surface and air temperatures

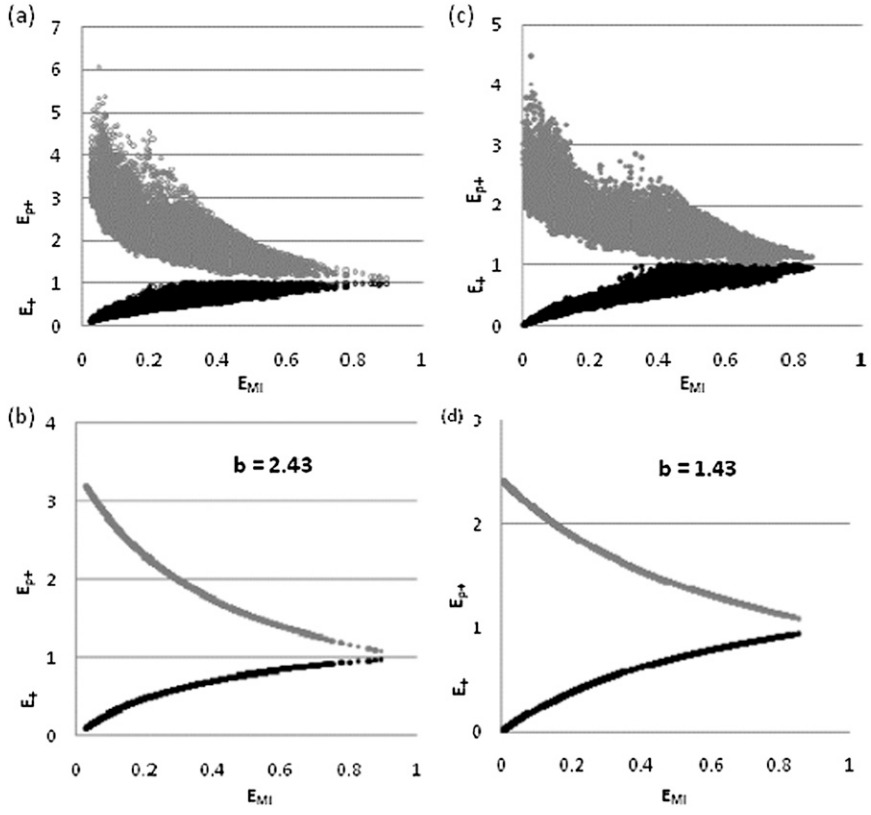

FIG. 7. (top) Normalized CR curves and (bottom) optimized theoretical CR curves for (a),(b) sagebrush and (c),(d) cheatgrass. Black circles indicate E_+ and gray circles indicate E_{P_+}.

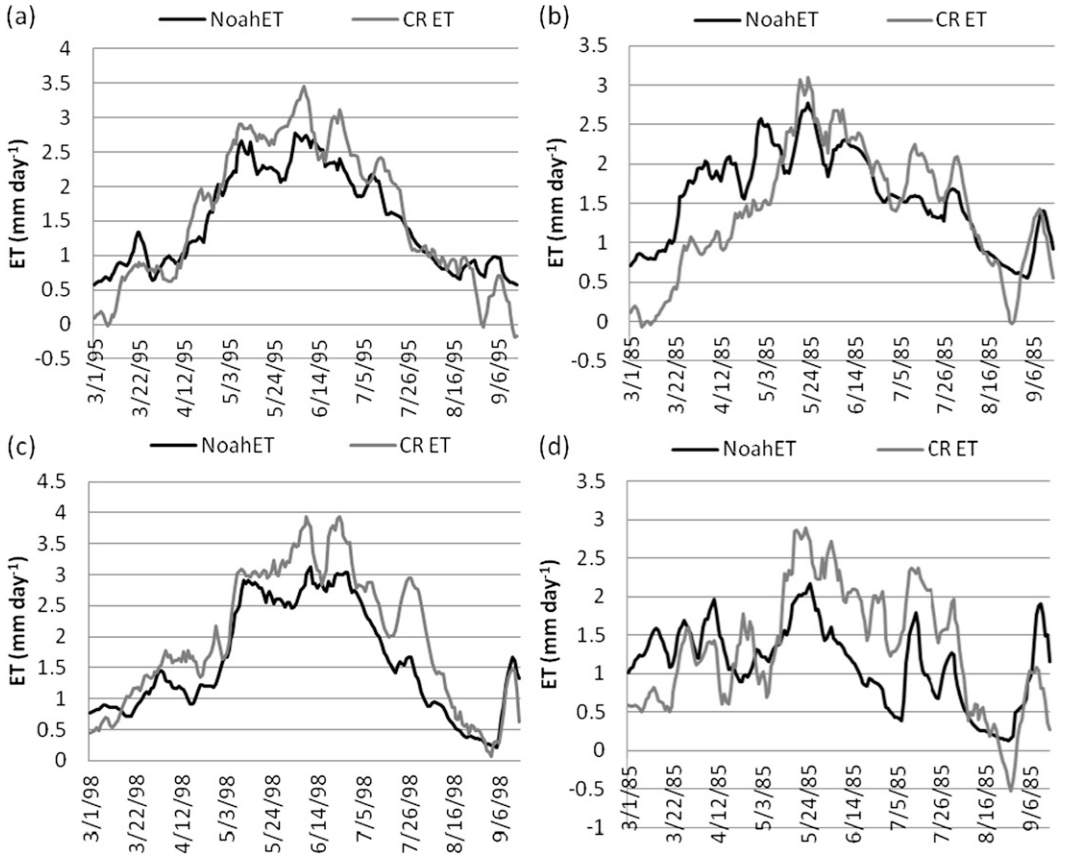

FIG. 8. Time series plots of ET (top) from sagebrush and (bottom) from cheatgrass showing the (a),(c) best-correlated and (b),(d) worst-correlated years. Black line denotes the ET_{Noah} and gray line is ET derived from CR (mm day^{-1}).

where net advection is present, similar to an ''oasis'' effect. In that situation, more ambient energy than available energy is present because of advection, and there is no increase in humidity at a regional scale to reduce the measured or estimated ET_p. The theoretical CR curves achieved convergence when E_{MI} reached 1 (unity) at the sagebrush site but not at the cheatgrass site. According to Figs. 5c,f, E_{MI} was close to 1 (unity) over the sagebrush site at the end of November, and for the cheatgrass site, maximum E_{MI} was roughly 0.8. This could be explained by the fact that the soil moisture at the sagebrush site was consistently higher than at the cheatgrass site. The derived CR in this study for two sites was found to be

$$(1 + 2.43)\mathrm{ET}_w = \mathrm{ET}_p + 2.43 \times \mathrm{ET}_{\mathrm{Noah}}\,(\text{sagebrush}), \tag{13}$$

$$(1 + 1.43)\mathrm{ET}_w = \mathrm{ET}_p + 1.43 \times \mathrm{ET}_{\mathrm{Noah}}\,(\text{cheatgrass}). \tag{14}$$

c. Validation

Since the CR technique requires only the meteorological measurements, flux data, and spatially variable values of b to be applicable for other time periods, computation of actual ET from CR technique for a given location is relatively effective. Given the lack of field observations of ET over a large area, comparison of model-to-model estimates provides a useful framework for validating the NARR data and also reinforces the use of NARR forcings.

As a validation, it is important to check the applicability of CR derived for one time period to other time periods. After deriving independent values of b for two different vegetation types, sagebrush and cheatgrass, the CR-based Eqs. (13) and (14) were evaluated by applying them over the same sites for a different year to predict ET, which subsequently compared against the ET_{Noah}. Figure 8 is the time series plot of daily values of ET_{Noah} versus ET derived from the CR. ET from 1 March to 15 September was plotted, as b was derived for that period earlier to see if the derived relationship was still valid

TABLE 1. Statistics of the ET_{Noah} and ET derived from CR on a daily time scale. MBE is $\sum(ET_{Noah} - ET_{CR})/n$, where n is the total number of days.

	Sagebrush		Cheatgrass	
	RMSE (mm day^{-1})	MBE (mm day^{-1})	RMSE (mm day^{-1})	MBE (mm day^{-1})
March	0.43	0.31	0.59	0.36
April	0.38	−0.08	0.55	0.01
May	0.59	−0.48	0.61	−0.27
June	0.70	−0.60	0.76	−0.48
July	0.55	−0.47	0.77	−0.58
August	0.33	0.34	0.54	−0.23
Average	0.50	−0.24	0.64	−0.20

for a time period other than this period. We first computed 7-day moving averages of ET_{Noah} as well as ET_p and ET_w. Subsequently, ET was estimated [from Eqs. (13) and (14)] using 7-day moving averages of ET_p and ET_w, with the already-derived b values for sagebrush and cheatgrass. Figures 8a and 8b represent sagebrush, and Figs. 8c and 8d represent cheatgrass. Both sagebrush and cheatgrass sites showed a good agreement between ET_{Noah} and ET derived from CR, with an R^2 of 0.76 for sagebrush (Fig. 8a) and 0.80 for cheatgrass (Fig. 8c). Root-mean-square errors (RMSEs) computed between ET_{Noah} and CR-derived ET were 0.52 and 0.54 mm day^{-1}, and it is important to emphasize that the extent of uncertainties in these estimates could be partly attributed to NARR forcings and Noah LSM parameterization for this area. The negative mean bias errors (MBEs) are 0.19 and 0.01 mm day^{-1}. Monthly RMSEs showed that the minimum was in August for both sagebrush and cheatgrass (Table 1). Figure 9 shows the time series plots of ET for sagebrush and cheatgrass for one cell during 1 March through 31 August for the validation period between 1981 and 2000. Comparison of CR and ET_{Noah} showed the CR underestimated ET mostly during early spring and late fall. Overall, the peak estimates were in agreement between the CR and Noah-simulated ET. This was mainly because ET_p was higher than ET_w by more than a factor of 2, as observed by Huntington et al. (2011) for winter months. This condition reduced, or sometimes resulted in, negative ET, as seen in Fig. 8. The long-term trends in ET followed the dry years of the late 1980s and 1990s and the wet years of the mid-1990s. The Penman equation that was used to calculate ET_p did not perform well during the winter months, when the available energy was negative or very close to zero (Xu and Singh

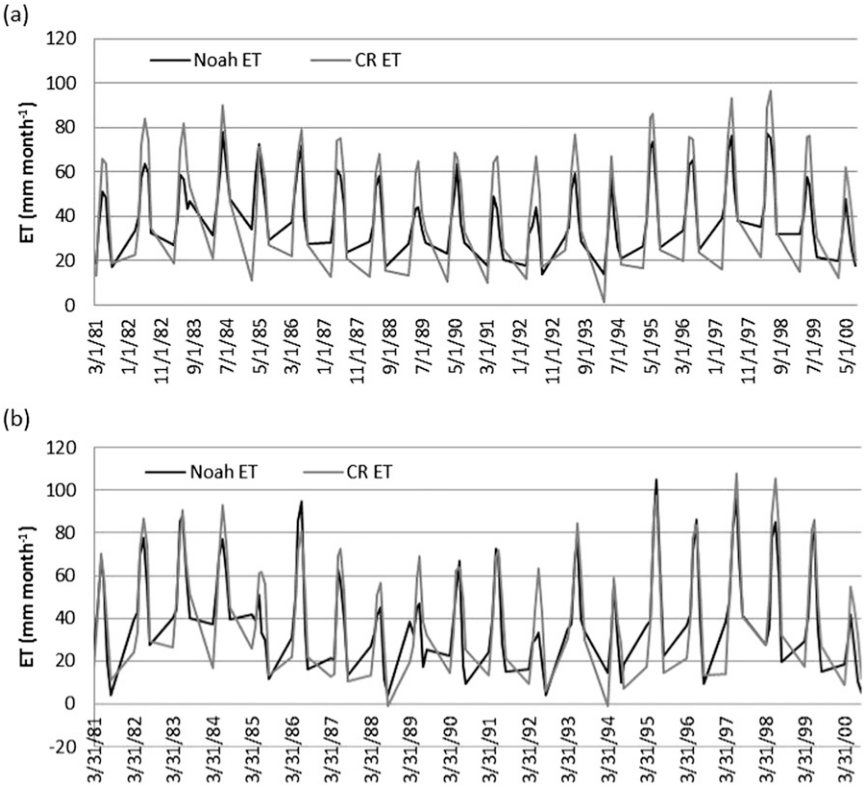

FIG. 9. Time series plots of monthly ET for (a) sagebrush and (b) cheatgrass from a single cell from each vegetation type from 1 Mar to 31 Aug for the validation period between 1981 and 2000. Black line denotes the ET_{Noah} and gray line represents ET_{CR} (mm month^{-1}).

2005). At the cheatgrass site, CR-derived ET was able to capture the seasonal and peak ET that closely agreed both in magnitude and time with the ET_{Noah}. The CR-derived ET at the sagebrush site showed great variations and missed both magnitude and timing of peak ET but generally captured the seasonal trend.

7. Summary and conclusions

Given the semiarid conditions and the importance of water for agriculture, hydropower, navigation, and ecosystem functions in the Snake River Plain of southern Idaho, evaluating water resources management and developing a better understanding of climate-driven hydrologic processes is necessary. Since ET is an important hydrologic process impacting soil moisture states and groundwater recharge and streamflow conditions, our ability to accurately estimate ET is critical for current and future climate conditions. However, temporal and spatial variations of ET in this area are limited by the lack of long-term meteorological and energy balance measurements.

To better understand spatial variability and potential atmospheric and land surface feedbacks and to test if a simple model could be used to predict ET, the Noah LSM-simulated fluxes, along with the NARR meteorological data, were used in derivation of the CR for the two main vegetation types in the area, grasslands and shrublands. Three-hourly NARR meteorological data were interpolated into hourly data in the HRLDAS platform. The results clearly indicated the complementarity between ET_{Noah} and the ET_p calculated from the NARR data. It was found that the CR was asymmetric for two vegetation types, with b values greater than unity. Noah LSM–simulated ET was used in this study for the lack of measured ET. When comparing simulated ET with field-measured ET for a short time period, it was noted that Noah LSM ET was overestimated during the summer months and slightly underestimated during the spring months. This could be a possible reason for the asymmetry seen in the CR. Furthermore, Pettijohn and Salvucci (2009) reported that the poor representation of the drying trends for this region by the Penman method, which was used to compute ET_p, could also contribute to the asymmetric behavior. The CR, derived for 2001–10, was applied for a 20-yr period between 1981 and 2000 to validate the approach. The validation showed high correlation coefficients but large errors. In general, ET derived from CR captured the general trends of ET compared to ET_{Noah}, proving that the CR can be applied to estimate ET in these natural vegetation ecosystems. In addition to demonstrating this well-established CR theory to estimate ET for the natural vegetation domain in Idaho, this study also provided a validation mechanism to evaluate the NARR data in a very different aspect. Also, when field observations are present, CR derived using field observations would be able to use to validate the ET rates in numerical models.

Acknowledgments. This research is supported by the National Science Foundation (NSF) Idaho Experimental Program to Stimulate Competitive Research (EPSCoR) and by the National Science Foundation under Award EPS-0814387. Partial support came from the National Oceanic and Atmospheric Administration (NOAA) via the Northwest Climate Decision Support Consortium (pnwclimate.org) under Award NA10OAR4310218. We also thank the two anonymous reviewers and the Editor, whose comments enormously improved the manuscript.

REFERENCES

Alfieri, J. G., X. Xiao, D. Niyogi, R. A. Pielke, F. Chen, and M. A. LeMone, 2009: Satellite-based modeling of transpiration from the grassland in the southern Great Plains, USA. *Global Planet. Change,* **67,** 78–86.

Allen, R. G., and Coauthors, 2007a: Satellite-based energy balance for mapping evapotranspiration with internal calibration (METRIC)—Applications. *J. Irrig. Drain. Eng.,* **133,** 395–406.

——, M. Tasumi, and R. Trezza, 2007b: Satellite-based energy balance for mapping evapotranspiration with internal calibration (METRIC)—Model. *J. Irrig. Drain. Eng.,* **133,** 380–394.

Avissar, R., and R. A. Pielke, 1991: The impact of plant stomatal control on mesoscale atmospheric circulations. *Agric. For. Meteor.,* **54,** 353–372.

Barnett, T. P., J. C. Adam, and D. P. Lettenmaier, 2005: Potential impacts of a warming climate on water availability in snow-dominated regions. *Nature,* **438,** 303–309.

Betts, A. K., F. Chen, K. E. Mitchell, and Z. Janjic, 1997: Assessment of the land surface and boundary layer models in the two operational versions of the NCEP Eta model using FIFE data. *Mon. Wea. Rev.,* **125,** 2896–2916.

Beyrich, F., H. De Bruin, W. Meijninger, J. Schipper, and H. Lohse, 2002: Results from one-year continuous operation of a large aperture scintillometer over a heterogeneous land surface. *Bound.-Layer Meteor.,* **105,** 85–97.

Bouchet, R. J., 1963: Évapotranspiration réelle et potentielle signification climatique. International Association of Scientific Hydrology Publ. 62, 134–142.

Brutsaert, W., and H. Stricker, 1979: An advection-aridity approach to estimate actual regional evapotranspiration. *Water Resour. Res.,* **15,** 443–450.

——, and M. B. Parlange, 1998: Hydrologic cycle explains the evaporation paradox. *Nature,* **396,** 30.

Bureau of Reclamation, 2011: Reclamation: SECURE Water Act section 9503(c)—Reclamation climate change and water 2011. Rep. to Congress, U.S. Dept. of the Interior, Denver, CO, 226 pp.

Chen, F., and Coauthors, 1996: Modeling of land surface evaporation by four schemes and comparison with FIFE observations. *J. Geophys. Res.,* **101,** 7251–7268.

——, Z. Janjic, and K. Mitchell, 1997: Impact of atmospheric surface-layer parameterization in the new land–surface scheme of the NCEP mesoscale Eta model. *Bound.-Layer Meteor.,* **85,** 391–421.

——, D. N. Yates, H. Nagai, M. A. Lemone, K. Ikeda, and R. L. Grossman, 2003: Land surface heterogeneity in the Cooperative Atmosphere Surface Exchange Study (CASES-97). Part I: Comparing model surface flux maps with surface-flux tower and aircraft measurements. *J. Hydrometeor.,* **4,** 196–218.

——, and Coauthors, 2007: Description and evaluation of the characteristics of the NCAR high-resolution land data assimilation system. *J. Appl. Meteor. Climatol.,* **46,** 694–713.

Clark, G. M., 2010: Changes in patterns of streamflow from unregulated watersheds in Idaho, western Wyoming, and northern Nevada. *J. Amer. Water Resour. Assoc.,* **46,** 486–497, doi:10.1111/j.1752-1688.2009.00416.x.

Crago, R. D., R. J. Qualls, and M. Feller, 2010: A calibrated advection-aridity evaporation model requiring no humidity data. *Water Resour. Res.,* **46,** W09519, doi:10.1029/2009WR008497.

Ek, M. B., K. E. Mitchell, Y. Lin, E. Rogers, P. Grunmann, V. Koren, G. Gayno, and J. D. Tarpley, 2003: Implementation of Noah land surface model advances in the National Centers for Environmental Prediction operational mesoscale Eta model. *J. Geophys. Res.,* **108,** 8851, doi:10.1029/2002JD003296.

Granger, R. J., and D. M. Gray, 1989: Evaporation from natural nonsaturated surfaces. *J. Hydrol.,* **111,** 21–29.

Hobbins, M. T., J. A. Ramírez, and T. C. Brown, 2001: The complementary relationship in estimation of regional evapotranspiration: An enhanced advection-aridity model. *Water Resour. Res.,* **37,** 1389–1403.

——, ——, and ——, 2004: Trends in pan evaporation and actual evapotranspiration across the conterminous U.S.: Paradoxical or complementary? *Geophys. Res. Lett.,* **31,** L13503, doi:10.1029/2004GL019846.

Huntington, J. L., J. Szilagyi, S. W. Tyler, and G. M. Pohll, 2011: Evaluating the complementary relationship for estimating evapotranspiration from arid shrublands. *Water Resour. Res.,* **47,** W05533, doi:10.1029/2010WR009874.

Jin, J., and N. L. Miller, 2007: An analysis of the impact of snow on daily weather variability in mountainous regions using MM5. *J. Hydrometeor.,* **8,** 245–258.

Jin, X., and V. Sridhar, 2012: Impacts of climate change on hydrology and water resources in the Boise and Spokane River basins. *J. Amer. Water Resour. Assoc.,* **48,** 197–220, doi:10.1111/j.1752-1688.2011.00605.x.

Kahler, D. M., and W. Brutsaert, 2006: Complementary relationship between daily evaporation in the environment and pan evaporation. *Water Resour. Res.,* **42,** W05413, doi:10.1029/2005WR004541.

Kavvas, M. L., Z. Q. Chen, L. Tan, S.-T. Soong, A. Terakawa, J. Yoshitani, and K. Fukami, 1998: A regional-scale land surface parameterization based on areally-averaged hydrological conservation equations. *Hydrol. Sci. J.,* **43,** 611–631.

Kjelstrom, L. C., 1995: Streamflow gains and losses in the Snake River and ground-water budgets for the Snake River Plain, Idaho and eastern Oregon. U.S. Geological Survey Professional Paper 1408-C, 47 pp. [Available online at http://pubs.usgs.gov/pp/1408c/report.pdf.]

Koren, V., J. C. Schaake, K. E. Mitchell, Q. Y. Duan, F. Chen, and J. Baker, 1999: A parameterization of snowpack and frozen ground intended for NCEP weather and climate models. *J. Geophys. Res.,* **104,** 19 569–19 585.

Luo, Y., E. H. Berbery, K. E. Mitchell, and A. K. Betts, 2007: Relationship between land surface and near-surface atmospheric variables in the NCEP North American Regional Reanalysis. *J. Hydrometeor.,* **8,** 1184–1203.

Meijninger, W. M. L., F. Beyrich, A. Luedi, W. Kohsiek, and H. A. R. De Bruin, 2006: Scintillometer-based turbulent fluxes of sensible and latent heat over a heterogeneous land surface—A contribution to LITFASS-2003. *Bound.-Layer Meteor.,* **121,** 89–110.

Mesinger, F., and Coauthors, 2006: North American Regional Reanalysis. *Bull. Amer. Meteor. Soc.,* **87,** 343–360.

Mitchell, K. E., and Coauthors, 2004: The multi-institution North American Land Data Assimilation System (NLDAS): Utilizing multiple GCIP products and partners in a continental distributed hydrological modeling system. *J. Geophys. Res.,* **109,** D07S90, doi:10.1029/2003JD003823.

Monteith, J. L., 1973: *Principles of Environmental Physics.* Elsevier, 241 pp.

——, 1975: *Vegetation and the Atmosphere Case Studies*. Academic Press, 278 pp.

Morton, F. I., 1983: Operational estimates of areal evapotranspiration and their significance to the science and practice of hydrology. *J. Hydrol.,* **66,** 1–76.

Mote, P. W., 2006: Climate-driven variability and trends in mountain snowpack in western North America. *J. Climate,* **19,** 6209–6220.

Oudin, L., C. Michel, V. Andréassian, F. Anctil, and C. Loumagne, 2005: Should Bouchet's hypothesis be taken into account in rainfall-runoff modeling? An assessment over 308 catchments. *Hydrol. Processes,* **19,** 4093–4106.

Ozdogan, M., G. D. Salvucci, and B. T. Anderson, 2006: Examination of the Bouchet–Morton complementary relationship using a mesoscale climate model and observations under a progressive irrigation scheme. *J. Hydrometeor.,* **7,** 235–251.

Pan, H. L., and L. Mahrt, 1987: Interaction between soil hydrology and boundary layer development. *Bound.-Layer Meteor.,* **38,** 185–202.

Penman, H. L., 1948: Natural evaporation from open water, bare soil and grass. *Proc. Roy. Soc. London,* **193A,** 120–146.

Pettijohn, J. C., and G. D. Salvucci, 2009: A new two-dimensional physical basis for the complementary relation between terrestrial and pan evaporation. *J. Hydrometeor.,* **10,** 565–574.

Priestley, C. H. B., and R. J. Taylor, 1972: On the assessment of surface heat flux and evaporation using large-scale parameters. *Mon. Wea. Rev.,* **100,** 81–92.

Radell, D. B., and C. M. Rowe, 2008: An observational analysis and evaluation of land surface model accuracy in the Nebraska Sand Hills. *J. Hydrometeor.,* **9,** 601–621.

Rana, G., and N. Katerji, 2000: Measurement and estimation of actual evapotranspiration in the field under Mediterranean climate: A review. *Eur. J. Agron.,* **13,** 125–153.

Raupach, M. R., 1998: Influence of local feedbacks on land–air exchanges of energy and carbon. *Global Change Biol.,* **4,** 477–494.

Samain, B., B. V. A. Ferket, W. Defloor, and V. R. N. Pauwels, 2011: Estimation of catchment averaged sensible heat fluxes using a large aperture scintillometer. *Water Resour. Res.,* **47,** W05536, doi:10.1029/2009WR009032.

Schaake, J. C., V. I. Koren, Q.-Y. Duan, K. E. Mitchell, and F. Chen, 1996: Simple water balance model for estimating runoff at different spatial and temporal scales. *J. Geophys. Res.,* **101,** 7461–7475.

Shukla, S., A. C. Steinemann, and D. P. Lettenmaier, 2011: Drought monitoring for Washington state: Indicators and applications. *J. Hydrometeor.,* **12,** 66–83.

Sridhar, V., and A. Nayak, 2010: Implications of climate-driven variability and trends for the hydrologic assessment of the Reynolds Creek Experimental Watershed, Idaho. *J. Hydrol.,* **385,** 183–202.

——, R. L. Elliott, F. Chen, and J. A. Brotzge, 2002: Validation of the NOAH-OSU land surface model using surface flux measurements in Oklahoma. *J. Geophys. Res.,* **107,** 4418, doi:10.1029/2001JD001306.

——, ——, and ——, 2003: Scaling effects on modeled surface energy balance components using the Noah land surface model. *J. Hydrol.,* **280,** 105–123.

Szilagyi, J., 2007: On the inherent asymmetric nature of the complementary relationship of evaporation. *Geophys. Res. Lett.,* **34,** L02405, doi:10.1029/2006GL028708.

——, and J. Jozsa, 2008: New findings about the complementary relationship-based evaporation estimation methods. *J. Hydrol.,* **354,** 171–186.

——, M. Hobbins, and J. Jozsa, 2009: A modified advection-aridity model of evapotranspiration. *J. Hydrol. Eng.,* **14,** 569–574.

Tang, Q., S. Peterson, R. H. Cuenca, Y. Hagimoto, and D. P. Lettenmaier, 2009: Satellite-based near-real-time estimation of irrigation crop water consumption. *J. Geophys. Res.,* **114,** D05114, doi:10.1029/2008JD010854.

Tang, R., Z.-L. Li, and B. Tang, 2010: An application of the T_s–VI triangle method with enhanced edges determination for evapotranspiration estimation from MODIS data in arid and semi-arid regions: Implementation and validation. *Remote Sens. Environ.,* **114,** 540–551.

van Heerwaarden, C. C., J. V. G. de Arellano, and A. J. Teuling, 2010: Land-atmosphere coupling explains the link between pan evaporation and actual evapotranspiration trends in a changing climate. *Geophys. Res. Lett.,* **37,** L21401, doi:10.1029/2010GL045374.

Walter, M. T., D. S. Wilks, J. Y. Parlange, and R. L. Schneider, 2004: Increasing evapotranspiration from the conterminous United States. *J. Hydrometeor.,* **5,** 405–408.

Xu, C.-Y., and V. P. Singh, 2005: Evaluation of three complementary relationship evapotranspiration models by water balance approach to estimate actual regional evapotranspiration in different climatic regions. *J. Hydrol.,* **308,** 105–121.

Yang, D., F. Sun, Z. Liu, Z. Cong, and Z. Lei, 2006: Interpreting the complementary relationship in non-humid environments based on the Budyko and Penman hypotheses. *Geophys. Res. Lett.,* **33,** L18402, doi:10.1029/2006GL027657.